From retrodiction to Bayesian quantum imaging

2017 J. Opt. 19 044001

(http://iopscience.iop.org/2040-8986/19/4/044001)

OPEN ACCESS
IOP Publishing
Journal of Optics
J. Opt. 19 (2017) 044001 (7pp)
https://doi.org/10.1088/2040-8986/aa5ccf

From retrodiction to Bayesian quantum imaging

Fiona C Speirits[1], **Matthias Sonnleitner and Stephen M Barnett**

School of Physics and Astronomy, University of Glasgow, Glasgow G12 8QQ, United Kingdom

E-mail: fiona.speirits@glasgow.ac.uk

Received 13 December 2016, revised 24 January 2017
Accepted for publication 30 January 2017
Published 3 March 2017

Abstract

We employ quantum retrodiction to develop a robust Bayesian algorithm for reconstructing the intensity values of an image from sparse photocount data, while also accounting for detector noise in the form of dark counts. This method yields not only a reconstructed image but also provides the full probability distribution function for the intensity at each pixel. We use simulated as well as real data to illustrate both the applications of the algorithm and the analysis options that are only available when the full probability distribution functions are known. These include calculating Bayesian credible regions for each pixel intensity, allowing an objective assessment of the reliability of the reconstructed image intensity values.

Keywords: quantum imaging, Poisson noise, Bayesian inference, image denoising

(Some figures may appear in colour only in the online journal)

1. Introduction

Much of what we do in physics and, indeed, in other fields is about prediction: we seek to answer questions of the form 'what will happen if?'. Some problems and fields of endeavour, such as forensic science, archaeology and also image processing are fundamentally different in that they ask questions about earlier events: 'who committed the crime?', 'what destroyed this civilisation?' or, of more significance for this special issue, 'what is this an image of?'. To address each of these we start with what we know now and try to infer how we got to this situation. In this sense they each require retrodiction [1–4] or postdiction [5], the ability to infer something about the past, rather than prediction of the future.

Both predictions and retrodictions are usually probabilistic statements. Consider two possible events a and b that are perhaps correlated in some way, with a preceding b. A prediction might give the probability of b *given* that a occurred: $P(b|a)$. A retrodiction, however, would give the probability that a occurred given b: $P(a|b)$. These two conditional probabilities are related by Bayes' rule [6–10]:

$$P(b|a) = \frac{P(a|b)P(b)}{P(a)}. \tag{1}$$

This relationship hints at a link between retrodictive reasoning and Bayesian methods and it is this link that we seek to exploit in our study of quantum imaging. The connection between quantum retrodiction and Bayes' rule is, in fact, a profound one, in that it is possible to *derive* retrodictive quantum theory from the conventional predictive quantum theory and Bayes' rule [11].

At the heart of our approach is the retrodictive quantum theory of the photodetection process, applied to low light levels [12]. This provides a *pre-measurement* state based on the number of photocounts registered at a detector. At the simplest level, recording a single photocount will correspond to a single-photon pre-detection state. In practice, however, the pre-measurement state will be a mixed state on account of the imperfections in the detection process: finite detection efficiency and dark counts.

We seek to combine quantum retrodiction with Bayesian methods to obtain practical methods for image reconstruction at low light levels. In doing so, we note the existence of an impressive set of existing techniques for this important task [13–18] and hope that our retrodiction-based approach might

[1] Author to whom any correspondence should be addressed.

usefully add to these [19]. We begin, in section 2, with an explanation of quantum retrodiction methods before presenting the details of our algorithm in section 3. The results of applying this algorithm to both simulated and real data are reported in section 4 followed by a brief discussion of both the capabilities of our method as well as potential applications in section 5.

2. Quantum retrodiction

Quantum retrodiction may not be as familiar as its more commonly employed predictive counterpart and so a brief introduction to the main ideas may be of value. A more complete introduction may be found in [4]. To illustrate the principle, let us consider a simple quantum communications problem in which one party, Alice, sends to a second individual, Bob, a quantum system. Let Alice choose to prepare this in one of a complete set of orthonormal states $\{|i\rangle\}$ at time t_0. The system evolves under the evolution of its Hamiltonian and then, at time t_1, Bob performs a measurement of an observable with a *non-degenerate* complete set of eigenstates $\{|f\rangle\}$.

The evolution of the state between the preparation and measurement events is governed by the Schrödinger equation, the solution of which is

$$|i(t)\rangle = \hat{U}(t, t_0)|i\rangle, \tag{2}$$

where, for a time-independent Hamiltonian, the unitary operator $\hat{U}(t, t_0)$ is $\exp[-\mathrm{i}(t - t_0)\hat{H}/\hbar]$. If Alice prepared the state $|i\rangle$ then the probability that Bob's measurement gives the result corresponding to the state $|f\rangle$ is

$$P(f|i) = |\langle f|\hat{U}(t_1, t_0)|i\rangle|^2. \tag{3}$$

Let us analyse the situation from Bob's point of view. For him, he knows the outcome of his measurement and seeks to determine, from it, the state selected by Alice. In the absence of any other information, Bob assigns to each of the possible states available to Alice, $\{|i\rangle\}$, the same *a priori* probability (in line with the dictates of the principle of maximum entropy [20, 21]) and then application of Bayes' rule gives us the required conditional probability:

$$P(i|f) = |\langle i|\hat{U}^{\dagger}(t_1, t_0)|f\rangle|^2. \tag{4}$$

We have arrived at two conditional probabilities, $P(f|i)$ and $P(i|f)$, that are numerically equal but play very different roles: $P(f|i)$ is a *predictive* probability, suitable for use by Alice but $P(i|f)$ is a *retrodictive* probability suitable for use by Bob. It should be noted that these are numerically equal only because of the simplifying assumption that Bob has no prior information about Alice's choice of prepared state. For Bob it is natural to solve for the evolution of the state by starting with the *final* state $|f\rangle$ and integrating the Schrödinger equation backwards in time towards Alice's state preparation event. It is the idea of assigning the pre-measurement state on the basis of a later event (rather than an earlier one) that is the defining characteristic of quantum retrodiction[2].

It is important to emphasise that adopting a retrodictive approach does not give any different predictions to a correctly applied combination of conventional predictive quantum theory combined with Bayesian techniques. It has been valuable, however, in simplifying calculations and, more importantly, suggesting possibilities and ideas that are not readily apparent in the more familiar predictive approach. Striking examples include a novel class of generalised measurements [24, 25], quantum information processing in the past [26] and the quantum scissors device [27, 28] and the field of noiseless amplification that it led to [29–33]. In the context of quantum imaging, it has provided a novel analysis of entangled photon ghost imaging [34] including a justification for the Klyshko interpretation of the phenomenon [35].

The imaging problems we address here relate to reconstructing an image from photocounts registered in a pixel array, such as that provided by an electron multiplying charged coupled device. For each of the pixels we record an integer number of counts and it is these, and the correlations between the pixels, that form the basis for our image reconstruction. We can use quantum retrodiction to assign a pre-measurement state to the field impinging on each pixel. Let us focus on just a single pixel and let this have a quantum efficiency η, so that each photon results in a registered photocount with probability η [36, 37]. The retrodicted state corresponding to n photocounts is simply that produced by linear amplification of the state with gain $1/\eta$. The result is a mixed state, diagonal in the number-state basis. Based solely on the detection of m photocounts, the probability that the pre-measurement field had n photons is [25]

$$P(n_{\mathrm{photons}}|m_{\mathrm{counts}}) = \frac{n!}{m!(n-m)!}\eta^{m+1}(1-\eta)^{n-m}. \tag{5}$$

Note, in particular, that the probability distribution given no photocounts is peaked at 0 but has the form of a Bose–Einstein distribution:

$$P(n_{\mathrm{photons}}|0_{\mathrm{counts}}) = \eta(1-\eta)^n, \tag{6}$$

with a mean photon number $\bar{n} = \eta^{-1} - 1$. We can incorporate the additional imperfection of dark counts into this

[2] The intriguing feature of the amplitudes appearing in our two conditional probabilities is that there is no special time (perhaps a 'state-collapse' time) appearing and that we can write the amplitude in the form:

$$\langle f|\hat{U}(t_1, t_0)|i\rangle = \langle f|\hat{U}(t_1, t)\hat{U}(t, t_0)|i\rangle = \langle f(t)|i(t)\rangle,$$

where t is any time between t_0 and t_1, which we can associate with a Copenhagen-interpretation collapse time, although it is certainly not required that we do so [22]. The amplitude is manifestly independent of t and we can use this to obtain an evolution equation for $|f(t)\rangle$:

$$\frac{\mathrm{d}}{\mathrm{d}t}\langle f|\hat{U}(t_1, t_0)|i\rangle = 0 = \langle f(t)|\left(-\frac{\mathrm{i}}{\hbar}\hat{H}|i(t)\rangle\right) + \langle f(t)|i(t)\rangle$$
$$\Rightarrow \mathrm{i}\hbar\frac{\mathrm{d}}{\mathrm{d}t}|f(t)\rangle = \hat{H}|f(t)\rangle.$$

This retrodictive state satisfies the same Schrödinger equation as its predictive counterpart, $|i(t)\rangle$, but with the crucial difference that we solve for the retrodictive state with a *final* boundary condition rather than an initial one [23].

description [25]. The retrodictive state of the pre-measurement light field takes *no account* of any prior information, such as the average light level and the counts registered in adjacent pixels. Incorporating these presents no fundamental difficulty but is most naturally presented using methods of Bayesian analysis, as will be described in the remainder of this paper.

There is one further point that should be emphasised, however, and this is that determining the pre-measurement photon number is not our primary objective; rather we wish to determine a value to associate with the image for each pixel. These numbers will constitute our reconstructed (classical) image. This means that we have to contend not simply with detector imperfections but also with the intrinsic (Poissonian) spread in the photon number associated with the quantum shot noise for the light.

3. Bayesian quantum imaging with dark counts

Standard image denoising algorithms result in a single image output, with no metric to enable the user to judge either the quality of the reconstruction as a whole or the ability of the algorithm to deal with specific features within the image. Retrodictive denoising, however, returns both a final image and a posterior probability distribution at each pixel. This, combined with the ease of incorporating informed priors into the algorithm, provides information that is otherwise unobtainable with traditional image processing methods.

The motivation behind a Bayesian approach to image reconstruction and analysis comes in two parts. Firstly, it allows us the ability to include other information, in the form of priors, in addition to the raw data from each pixel. It also enables us to update our state of knowledge with new data. These key ingredients allow us to calculate the full posterior probability distributions and appropriate error bars at each image pixel.

To illustrate the power of retrodictive denoising, we present a statistically robust method for reconstructing an image generated from single photon counting by a photodetector with detection efficiency $0 < \eta \leqslant 1$ and performance-limited by a dark count rate $\epsilon \geqslant 0$, assumed to be the same for all pixels. In this regime, the probability of getting m_s discrete photocounts in a specified pixel from a time-integrated intensity λ is given by a Poisson distribution [38]

$$p(m_s|\lambda) = \mathrm{e}^{-\eta\lambda}\frac{(\eta\lambda)^{m_s}}{m_s!}. \tag{7}$$

For a well-calibrated detector, the equivalent probability of m_d dark counts is also given by a Poisson distribution $p(m_\mathrm{d}|\epsilon) = \mathrm{Pois}(m_\mathrm{d};\,\epsilon)$. It follows that the combined distribution for the total number of counts $m = m_s + m_\mathrm{d}$ is also Poissonian: $p(m|\lambda,\,\epsilon) = \mathrm{Pois}(m;\,\eta\lambda + \epsilon)$.

Following Bayes' rule (1), we can combine with the data a prior expectation that the intensity λ should, on average, be close to some value $\tilde{\lambda}$, in order to construct a probability distribution for the intensity at a single pixel $p(\lambda|m,\,\tilde{\lambda})$, such that

$$p(\lambda|m,\,\tilde{\lambda}) = \frac{p(m|\lambda)p(\lambda|\tilde{\lambda})}{p(m|\tilde{\lambda})}, \tag{8}$$

where $p(\lambda|\tilde{\lambda}) = \tilde{\lambda}^{-1}\exp(-\lambda/\tilde{\lambda})$ is the entropy maximising prior distribution, the normalisation factor $p(m|\tilde{\lambda}) = \int_0^\infty p(m|\lambda)p(\lambda)\,\mathrm{d}\lambda$ and we have omitted explicit reference to the dark count rate for conciseness i.e. $p(m|\lambda,\,\epsilon) \equiv p(m|\lambda)$.

Having considered the inclusion of priors, we now address the equally important use of Bayesian inference to update a probability distribution $p(\lambda|m,\,\tilde{\lambda})$ with new data m'. This can be iterated over a set of measurements $\mathcal{M} = \{m, m', m'', \ldots\}$, which allows us to retrodict their average intensity λ and construct a joint posterior probability distribution $p(\lambda|\mathcal{M},\,\tilde{\lambda})$. This, combined with the ability to incorporate informed priors, now allows us to optimise the image retrodiction.

3.1. Local retrodiction with local priors

Low photocount imaging provides a single measured image with typically less than one count per pixel and the average number of counts per pixel greater than the dark count rate, $\overline{m} > \epsilon$. In the simplest case we can follow equation (8) to construct the probability distribution for the intensity at the jth out of N_p pixels, λ_j. However, this can be improved upon by incorporating known attributes of typical images in order to produce a retrodicted probability distribution for each pixel that is informed by its surrounding neighbours. Given that the intensity varies smoothly across typical images, we can assume similar intensities at neighbouring pixels and therefore, for each pixel j, we combine a set of measurements $\mathcal{M}_j$ within a neighbourhood[3] of radius R_0, as depicted in figure 1. We also define a local prior for each pixel $\tilde{\lambda}_j$ by incorporating the ring of pixels surrounding the radius R_0, thus ensuring no pixel is double-counted. Simply choosing a prior $\tilde{\lambda}_j = (\overline{m} - \epsilon)/\eta$ would give a virtually uniform prior for all pixels in the image, which leads to a systematic discrepancy between the retrodicted expectation value and the true intensity, as discussed in previous work [19, 40]. Instead, we assume that the average intensity within this ring will be close to the true intensity of the central pixel, with one caveat: in very dark regions, the average number of counts in this ring may be less than the dark count rate, resulting in a negative prior. To avoid this we first use the average of all remaining pixels in the image, which we can expect to be larger than the dark count rate for a non-empty image, as a prior for the total intensity within the ring around pixel j. This returns a positive, local prior without using measurement values allocated for the actual retrodiction.

Combining the local retrodiction over a set of pixel measurements $\mathcal{M}_j$ from N_j pixels of total photocounts $M_j = \sum_{m\in\mathcal{M}_j} m$ with this local prior $\tilde{\lambda}_j$ then yields the full

[3] The assumption that all intensities are similar within a region of radius R_0 clearly fails for large R_0 or at edges where the intensity changes rapidly from one pixel to the next. However, the assumption is valid for the majority of an image, which is why it forms the basis of many common image denoising algorithms [39].

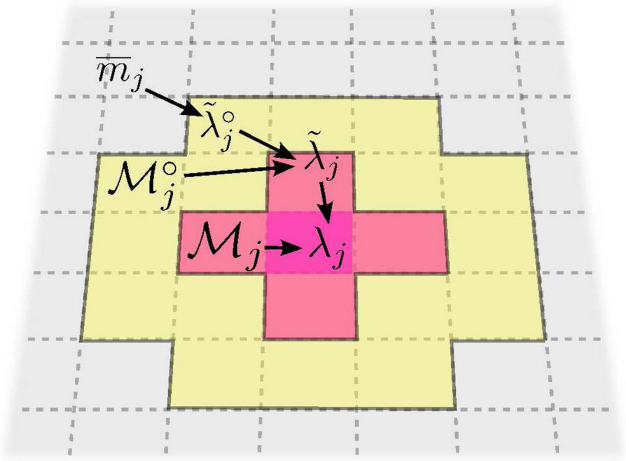

Figure 1. An illustration of local retrodiction with local priors. To retrodict the intensity λ_j at the central pixel we use all measurement data $\mathcal{M}_j$ within a radius $R_0 = 1$ (red). The prior $\tilde{\lambda}_j$ is generated using the data in $\mathcal{M}_j^\circ$ (yellow) and a further prior $\tilde{\lambda}_j^\circ$, which is generated using the average number of measurements in the rest of the image $\overline{m}_j = \overline{m} - (M_j - M_j^\circ)/N_\mathrm{p} \approx \overline{m}$ (grey). The flow of information is indicated by the arrows.

posterior probability distribution for the intensity at each pixel λ_j:

$$p(\lambda_j|\mathcal{M}_j, \tilde{\lambda}_j) = \eta\frac{(\eta\lambda + \epsilon)^{a-1}b^a}{\Gamma(a, \epsilon b)}\mathrm{e}^{-(\eta\lambda+\epsilon)b}, \tag{9}$$

where $a = M_j + 1$, $b = N_j + 1/(\eta\tilde{\lambda}_j)$ and $\Gamma(s, x) = \int_x^\infty t^{s-1}\mathrm{e}^{-t}\mathrm{d}t$ is the upper incomplete gamma function. The local prior

$$\tilde{\lambda}_j = \frac{1}{\eta}\left[\frac{\Gamma(\alpha + 1, \epsilon\beta)}{\beta\Gamma(\alpha, \epsilon\beta)} - \epsilon\right], \tag{10}$$

where $\alpha = M_j^\circ + 1$ and $\beta = N_j^\circ + 1/(\eta\tilde{\lambda}_j^\circ)$ uses data from the surrounding ring as indicated by the circle, while $\tilde{\lambda}_j^\circ \approx (\overline{m} - \epsilon)/\eta$.

The image is then constructed by selecting a given intensity value for each pixel from the corresponding distribution. This would normally, and intuitively, be the maximum likelihood value

$$\lambda_j = \frac{1}{\eta}\left(\frac{M_j}{b} - \epsilon\right). \tag{11}$$

However, in the low photocount regime there will be many pixels with fewer photocounts than dark counts. As such, a large fraction of the pixels will have a probability distribution with maximum likelihood value equal to zero (which occurs whenever $M_j < \epsilon b$). A more informative measure of the intensity is the expectation value of the distribution (9) at each pixel:

$$\mathbb{E}(\lambda_j|\mathcal{M}_j, \tilde{\lambda}_j) = \frac{1}{\eta}\left[\frac{a}{b} + \frac{(\epsilon b)^a}{b}\frac{\mathrm{e}^{-\epsilon b}}{\Gamma(a, \epsilon b)} - \epsilon\right]. \tag{12}$$

This value of the intensity at each pixel λ_j will then form our reconstructed image in figures 2, 3 and 5.

3.2. Goodness of fit

Retrodictive image denoising utilises Bayes' rule to combine data and prior information in order to produce a probability distribution for each pixel. It is therefore prudent to use the tools of Bayesian inference to assess the calculated distributions, and hence the reconstructed image. A common sampling theory approach [8] is to calculate confidence intervals for a given distribution using the mean and standard deviation σ to identify bounds at for example 1σ, 2σ or 3σ from the mean. In a frequentist interpretation, these indicate how often the so-called 'true' value would be expected to lie within a given bound over a large number of repeated measurements, in these cases 68.3%, 95.4% or 99.7% of the time (and indeed these bounds should enclose 68.3%, 95.4% or 99.7% of the distribution).

However, there are two significant issues with applying this approach to the analysis of a retrodicted image. The first is that these confidence intervals are only valid for a Gaussian distribution; the probability distribution for each pixel in our reconstructed image is similar to a gamma distribution and therefore the commonly defined confidence intervals do not enclose the correct fraction of the total distribution [20]. Secondly, and more importantly, it is meaningless to consider 'over repeated measurements' in this scenario as we have only one image to consider. We therefore turn to the Bayesian analogue of confidence intervals: credible regions. These are defined such that they bound a selected fraction of the distribution within the smallest possible range of parameter values. For ease of comparison this is often chosen to be 68.3%, 95.4% or 99.7%, but can be any selected percentage of the distribution, and these bounds are most readily understood as a measure of our degree of belief that the random parameter that we are attempting to evaluate, in this case the intensity, lies within these limits.

This interpretation does not rely on what would be measured in repeated samples and, most importantly, are applicable to *any* type of distribution. It should be noted that in the limit of large sample sizes (the central limit theorem) Bayesian credible regions and frequentist confidence intervals will overlap, as all distributions of independent variables with finite variance tend to a Gaussian limiting form [41]. These credible regions act as standard error bars in λ and allow some measure of how well the retrodicted probability distribution represents the true intensity value at each pixel.

4. Image retrodiction

We present three cases to illustrate our retrodictive denoising algorithm. The first two consist of simulated data and the third is photocount data from a ghost imaging experiment [15]. This range of images highlights both the strengths and weaknesses of our denoising algorithm and the extra analytical opportunities afforded by having the full probability distribution at each pixel. In the case of simulated data, we show an original image, the sampled data that acts as the 'measured' photocount data from an experiment and the

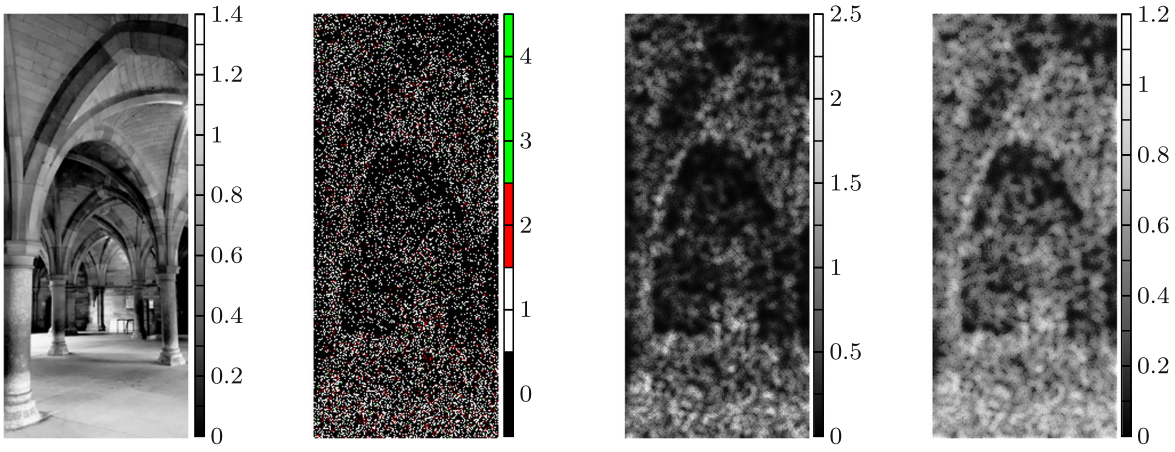

Figure 2. From left to right: the original image; the 'measured' low photocount data, sampled from the original image ($N_p = 372 \times 162$ pixels, detection rate $\eta = 0.3$, dark-count rate $\epsilon = 0.05$, on average $\overline{m} = 0.2$ counts per pixel); the reconstructed image produced by the local retrodiction algorithm ($R_0 = 3$), obtained by identifying the expectation value of the intensity λ at each pixel; the width of the 68.3% error bars in the retrodicted intensity λ.

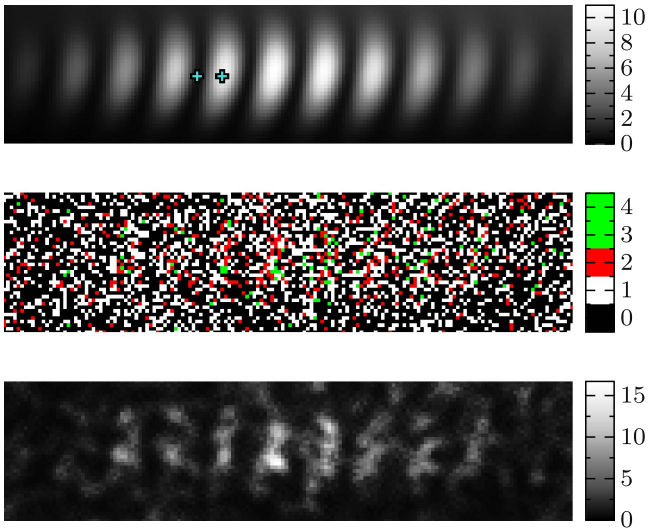

Figure 3. Top: the original image of simulated interference fringes. The crosses are pixels of interest used in figure 4. Middle: the 'measured' low photocount data, sampled from the original image ($N_p = 40 \times 160$, $\eta = 0.1$, $\epsilon = 0.3$, $\overline{m} = 0.5$). Bottom: the retrodicted intensity values, showing the reconstructed image ($R_0 = 1.5$).

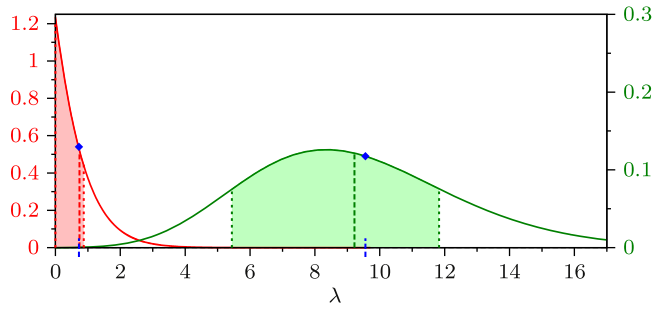

Figure 4. The probability distribution of the reconstructed intensities λ at each pixel of interest, as marked in figure 3, one dark (red, left vertical axis) and one bright (green, right vertical axis). This allows us to identify the error in λ from the width of the 68.3% credible region (shaded). We also show the expectation value (red or green dotted line) and the 'true' value of the intensity (blue dotted and diamond), which is only available when using simulated data from a known original image.

retrodicted image. In figure 2, we also show the width of the 68.3% credible regions at each pixel in order to illustrate the areas of the image that are more and less reliably reconstructed. It is evident that the algorithm returns the smallest spread in intensity probability for pixels in areas of a more uniform, lower intensity than at step changes to higher intensity areas. This is to be expected as the width of the probability distribution, and hence the credible regions, scales with the expectation value (12).

Reconstructing the full probability distribution function at each pixel allows credible regions to be assigned as error bars on the retrodicted intensity λ. In the case of interference fringes this can be used to assess the confidence of the identification of a dark or bright pixel, as shown in figures 3 and 4. This may have applications in measuring the fringe visibility and spacing from images when only a single, low intensity image is available.

Data from a low intensity ghost imaging experiment [15] is shown in figure 5, along with the retrodicted image and a further example of the statistical analysis allowed by this algorithm. In this case, we calculate the evidence that the estimated intensity at each pixel is larger than the median value of all the retrodicted expectation values λ_m across the image [9]

$$e(\lambda_j > \lambda_m|\mathcal{M}_j, \tilde{\lambda}_j) = 10\log_{10}\mathcal{O}(\lambda_j > \lambda_m|\mathcal{M}_j, \tilde{\lambda}_j), \quad (13)$$

where $\mathcal{O}(\lambda_j > \lambda_m|\mathcal{M}_j, \tilde{\lambda}_j)$ is the odds ratio for λ_j greater than the median value λ_m:

$$\mathcal{O}(\lambda > x|\mathcal{M}_j, \tilde{\lambda}_j) = \frac{\int_x^\infty p(\lambda'|\mathcal{M}_j\tilde{\lambda}_j)\mathrm{d}\lambda'}{\int_0^x p(\lambda'|\mathcal{M}_j\tilde{\lambda}_j)\mathrm{d}\lambda'}. \quad (14)$$

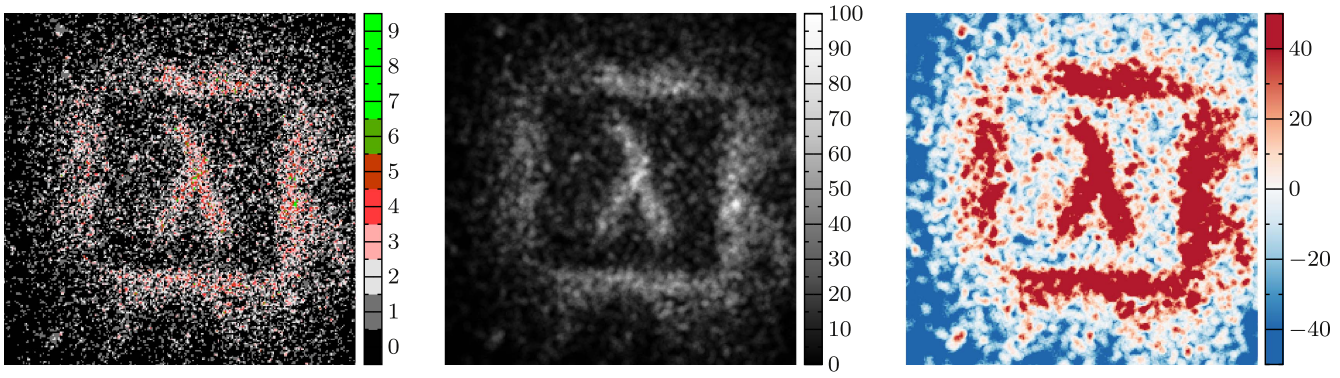

Figure 5. Left: real photocount data from a ghost experiment ($N_p = 240 \times 240$, $\eta = 0.05$, $\epsilon = 0.03$). Middle: the reconstructed image, showing the denoising applications of the retrodiction algorithm ($R_0 = 2.5$). Right: the evidence (in decibels) that the evaluated intensity at each pixel is above the retrodicted image median value, as given by equation (13).

This ratio of odds gives a measure of confidence in the algorithm's ability to differentiate between bright and dark areas, which is of particular interest when imaging an object with a simple structure such as figure 5. Moreover, it emphasises the areas in the reconstructed image of which we can be particularly confident in the identified intensity values i.e. the extrema values of the odds ratio.

5. Conclusions

We have presented the motivation for considering image reconstruction and denoising from a retrodictive perspective. The inherent links with Bayesian inference methods provides a natural framework for constructing an algorithm for analysis of low photocount data that is dominated by Poisson noise. A Bayesian approach also allows an objective appraisal of the quality of the resulting image and the analytical nature of the probability distribution functions negates the need for numerical methods such as Monte Carlo sampling.

There exist many conventional denoising algorithms that are suitable in most circumstances, except, we believe, in the limit of very sparse photocount data. It is in this regime that a probabilistic approach is essential in order to maximise the information that can be extracted from the data. We believe that these methods will have particular application in ghost imaging, as discussed in [15], imaging of fluorescent molecules and Bose–Einstein condensates, and non-photon Poisson statistic data, such as electron microscopy.

Acknowledgments

The authors would like to thank Reuben Aspden and Miles Padgett for kindly providing us with their experimental ghost imaging data. This work was supported by the EPSRC through the quantum hub QuantIC EP/M01326X/1, the Austrian Science Fund FWF (J 3703-N27) and the Royal Society (RP150122).

References

[1] Watanabe S 1955 Symmetry of physical laws: III. Prediction and retrodiction *Rev. Mod. Phys.* **27** 179
[2] Aharonov Y, Bergmann P G and Lebowitz J L 1964 Time symmetry in the quantum process of measurement *Phys. Rev.* **134** B1410–6
[3] Pegg D T and Barnett S M 1999 Retrodiction in quantum optics *J. Opt. B: Quantum Semiclass. Opt.* **1** 442
[4] Barnett S M 2014 *Quantum Retrodiction* (Cham: Springer) pp 1–30
[5] Belinfante F J 1975 *Measurements and Time Reversal in Objective Quantum Theory* (*International Series in Natural Philosophy*) (Oxford: Pergamon)
[6] Bayes M and Price M 1763 An essay towards solving a problem in the doctrine of chances. By the late Rev. Mr. Bayes, F. R. S. communicated by Mr. Price, in a letter to John Canton, A. M. F. R. S. *Phil. Trans.* **53** 370–418
[7] Jeffreys H 1961 *Theory of Probability* 3rd edn (Oxford: Oxford University Press)
[8] Box G E P and Tiao G C 1973 *Bayesian Inference in Statistical Analysis* (*Addison-Wesley Series in Behavioral Science: Quantitative Methods*) (Reading, MA: Addison-Wesley)
[9] Jaynes E T 2003 *Probability Theory, The Logic of Science* (Cambridge: Cambridge University Press)
[10] McGrayne S B 2011 *The Theory that Would Not Die: How Bayes Rule Cracked the Enigma Code, Hunted Down Russian Submarines, and Emerged Triumphant from Two Centuries of Controversy* (New Haven, CT: Yale University Press)
[11] Barnett S M, Pegg D T and Jeffers J 2000 Bayes' theorem and quantum retrodiction *J. Mod. Opt.* **47** 1779–89
[12] Barnett S M, Phillips L S and Pegg D T 1998 Imperfect photodetection as projection onto mixed states *Opt. Commun.* **158** 45–9
[13] Molina R, Núñez J, Cortijo F J and Mateos J 2001 Image restoration in astronomy: a Bayesian perspective *IEEE Signal Process. Mag.* **18** 11–29
[14] Bertero M, Boccacci P, Desiderà G and Vicidomini G 2009 Image deblurring with poisson data: from cells to galaxies *Inverse Problems* **25** 123006
[15] Morris P A, Aspden R S, Bell J E C, Boyd R W and Padgett M J 2015 Imaging with a small number of photons *Nat. Commun.* **6** 5913
[16] Le T, Chartrand R and Asaki T J 2007 A variational approach to reconstructing images corrupted by poisson noise *J. Math. Imaging Vis.* **27** 257–63
[17] Lefkimmiatis S, Maragos P and Papandreou G 2009 Bayesian inference on multiscale models for poisson intensity

estimation: applications to photon-limited image denoising *IEEE Trans. Image Process.* **18** 1724–41
[18] Shin D, Kirmani A, Goyal V K and Shapiro J H 2015 Photon-efficient computational 3D and reflectivity imaging with single-photon detectors *IEEE Trans. Comput. Imaging* **1** 112–25
[19] Sonnleitner M, Jeffers J and Barnett S M 2015 Image retrodiction at low light levels *Optica* **2** 950–7
[20] Jaynes E T and Kempthorne O 1976 *Confidence Intervals Versus Bayesian Intervals* (Dordrecht: Springer) pp 175–257
[21] Barnett S M 2009 *Quantum Information* (*Oxford Master Series in Physics*) (Oxford: Oxford University Press)
[22] Pegg D T 1993 Wave function collapse in atomic physics *Aust. J. Phys.* **46** 77
[23] Penfield R H 1966 More on the arrow of time *Am. J. Phys.* **34** 422–6
[24] Barnett S M and Pegg D T 1996 Phase measurement by projection synthesis *Phys. Rev. Lett.* **76** 4148–50
[25] Phillips L S, Barnett S M and Pegg D T 1998 Optical measurements as projection synthesis *Phys. Rev.* A **58** 3259–67
[26] Barnett S M, Jeffers J and Pegg D T 2003 Retrodictive quantum optics *Coherence and Quantum Optics VIII* (Boston, MA: Springer) pp 87–94
[27] Pegg D T, Phillips L S and Barnett S M 1998 Optical state truncation by projection synthesis *Phys. Rev. Lett.* **81** 1604–6
[28] Babichev S A, Ries J and Lvovsky A I 2003 Quantum scissors: teleportation of single-mode optical states by means of a nonlocal single photon *Europhys. Lett.* **64** 1
[29] Xiang G Y, Ralph T C, Lund A P, Walk N and Pryde G J 2010 Heralded noiseless linear amplification and distillation of entanglement *Nat. Photon.* **4** 7
[30] Ferreyrol F, Barbieri M, Blandino R, Fossier S, Tualle-Brouri R and Grangier P 2010 Implementation of a nondeterministic optical noiseless amplifier *Phys. Rev. Lett.* **104** 123603
[31] Jeffers J 2010 Nondeterministic amplifier for two-photon superpositions *Phys. Rev.* A **82** 12
[32] Eleftheriadou E, Barnett S M and Jeffers J 2013 Quantum optical state comparison amplifier *Phys. Rev. Lett.* **111** 213601
[33] Donaldson R J, Collins R J, Eleftheriadou E, Barnett S M, Jeffers J and Buller G S 2015 Experimental implementation of a quantum optical state comparison amplifier *Phys. Rev. Lett.* **114** 120505
[34] Tan E K, Jeffers J, Barnett S M and Pegg D T 2003 Retrodictive states and two-photon quantum imaging *Eur. Phys. J.* D **22** 495–9
Tan E K, Jeffers J, Barnett S M and Pegg D T 2004 *Eur. Phys. J.* D **29** 309 (erratum)
[35] Klyshko D N 1988 A simple method of preparing pure states of an optical field, of implementing the Einstein–Podolsky–Rosen experiment, and of demonstrating the complementarity principle *Sov. Phys.—Usp.* **31** 74
[36] Barnett S M, Pegg D T, Jeffers J, Jedrkiewicz O and Loudon R 2000 Retrodiction for quantum optical communications *Phys. Rev.* A **62** 022313
[37] Barnett S M, Pegg D T, Jeffers J and Jedrkiewicz O 2001 Master equation for retrodiction of quantum communication signals *Phys. Rev. Lett.* **86** 2455–8
[38] Loudon R 2000 *The Quantum Theory of Light* (Oxford: Oxford University Press)
[39] Buades A, Coll B and Morel J-M 2005 A review of image denoising algorithms, with a new one *Multiscale Model. Simul.* **4** 490–530
[40] Sonnleitner M, Jeffers J and Barnett S M 2016 Local retrodiction models for photon-noise-limited images *SPIE Photonics Europe* (International Society for Optics and Photonics) p 98960V
[41] MacKay D J C 2002 *Information Theory, Inference and Learning Algorithms* (New York: Cambridge University Press)